Control of Transition over Aerofoil Surfaces using Active Suction

Ahmadi-Baloutaki, M.[1], Sedaghat, A.[2], Saghafian, M.[3] and Badri, M. A[4*]
[1]PhD student, Department of Mechanical Engineering, University of Windsor, Ontario N9B 3P4, Canada. ahmadim@uwindsor.ca
[2]Assistant professor, Department of Mechanical Engineering, Isfahan University of Technology, Isfahan 84156-8311, Iran. Sedaghat@cc.iut.ac.ir
[3]Assistant professor, Department of Mechanical Engineering, Isfahan University of Technology, Isfahan 84156-8311, Iran. Saghafian@cc.iut.ac.ir
[4,*]Assistant professor, Research Institute for Subsea Science & Technology, Isfahan University of Technology, Isfahan 84156-8311, Iran.
malbdr@cc.iut.ac.ir (Corresponding author)

[Received date; Accepted date] – to be inserted later

ABSTRACT
The linear stability based on Orr-Sommerfeld equations and the e^N method was employed to determine the onset and control of transition over VFW-VF-2 and NACA65$_3$-018 aerofoil sections. For the VFW-VF-2 aerofoil, the effects of active suction on shock-boundary layer interaction were investigated. An enhanced lift to drag ratio was obtained for incidence angles below 6 degrees using suction coefficient as tiny as 0.0006. A parametric study were conducted to show the effects of the suction slot location, suction inclination angle and the extent of sucked flow through slots for flows around the NACA65$_3$-018 aerofoil. It was observed that transition was delayed regardless of suction positions. However, maximum delay in transition occurred when the sucked region was located between a critical point and the transition point. For all the cases studied here, lift to drag ratio was increased using active surface suction.

Key Words: Transition control; Laminar flow control; Active surface suction; Transonic; Aerofoil

1. INTRODUCTION

One of the methods to improve aerodynamic efficiency is to attain laminar flow over the wing surfaces which leads to lower frictional drag and consequently to lower fuel consumption. Attaining laminar flow, the velocity gradients and the corresponding shear stresses in boundary layer are much lower than its counterpart in turbulent boundary layers. The method for maintaining laminar boundary layer through using surface suction is referred to as Laminar Flow Control (LFC). Flow control is ability of active or passive manipulation of a flow field to achieve a desired change. LFC is an active boundary layer flow control (through suction) technique which is employed to maintain the laminar state beyond which the boundary layer is normally transitional or turbulent in the absence of control [1]. The principal types of active laminar flow control is surface cooling and removal of the boundary layer by suction through porous materials, multiple narrow surface slots or small perforations.

For the flow around an aerofoil, the purpose of control process is to achieve transition delay, separation postponement, lift enhancement, drag reduction, and noise suppression. Since the shear layer near the surface is removed with suction, this leads to elimination of viscosity effects and reduction of frictional drag. Due to suction, absolute pressure on the upper wing's surface decreases leading to lift enhancement [2]. Using suction, flow separation can also be postponed or removed by sucking the low energy fluid particles near the surface before these particles would have a chance to constitute a separation region. Flow suction also influences the stability of laminar boundary layers through two important effects. First, it reduces the thickness of boundary-layer and as known, thinner boundary layers is less prone to becoming turbulent. Secondly, it changes the shape of velocity profile which increases the critical Reynolds number, decreases the boundary layer thickness growth rates and narrows the band of frequencies receiving amplification [3].

The earliest experimental work on LFC for aircrafts was conducted in the late 1930s and 1940s primarily in wind tunnel. In 1939, some wind tunnel tests for the design of multiple suction slots were launched in NACA and produced the first aerodynamic criteria for obtaining laminar flow up to a length Reynolds number of 7 millions, a phenomenally large value at that time. In 1996, Bobbitt [4] published the results of their investigations on LFC at Langley 8-Foot Transonic Pressure Tunnel. They noted that, for the slot suction LFC test, full-chord laminar flow was obtained on the upper and lower surfaces for a chord Reynolds number of 10 million and drag reduction of about 60% was realized. According to them, increasing the Mach number had a stabilizing influence on the boundary layer instabilities and the transition location moved downstream. The majority of flow control design processes heavily depended on trial and error and designers' knowledge and intuition. Huang [5] accomplished a successful optimization of flow control on NACA0012 aerofoil using Genetic Algorithm. They determined the reasonable optimum control values within the control parameter range.

In 2005, Atik [6] did a series of numerical simulations to explore the effect of suction and suction/blowing as control mechanisms of leading-edge separation at high Reynolds number and achieved substantial delays in separation. They obtained unsteady boundary-layer solutions using a combination of Eulerian and Lagrangian techniques for an aerofoil at an angle-of-attack exceeding the critical value. It should be noted that when the angle of attack for a solid airfoil exceeds a certain critical value, the boundary layer in the leading-edge region is separated in a process known to lead to dynamic stall. In fact, in their work suction near the leading edge was studied in order to control separation and thereby inhibiting dynamic stall. The effects of various parameters associated with the finite length of suction and injection slots, their locations and the suction strength were considered. They mentioned that, when both suction and injection were applied together, the separation process was inhibited but the results were not as impressive as the results obtained by suction alone.

After years, the novel topic about LFC was stability of laminar flow. Many researchers studied the flow instabilities especially 2D type disturbances (Tollmein-Schlichtling waves) and their influence on laminar flow which was obtained by suction. Some of the works on LFC have been focused on finding the optimal suction distribution in surface slots. One of these works was performed by Pralits and Hanifi [7]. They used the optimal control theory and minimized an objective function based on a sum of the kinetic energy of an arbitrary number of disturbances for computing the optimal steady suction distribution in order to minimize the growth of convectively unstable disturbances and thus delayed laminar-turbulent transition on swept wings. Results presented in their work were claimed to be practicable for medium range commercial aircrafts.

Recently, Godarzi [8] has studied the concept of active flow control using a blowing jet over NACA0015 aerofoil's upper surface at Re = 455000 in different high angles of attack using FLUENT. His simulation results show that the blowing will increase the amount of lift and reduce drag. Also at high angles of attack, the blowing delay separation and improve the performance of the aerofoil. Godarzi [9] also studied flow control over NACA0012 aerofoil in different angles of attacks with three different suction ratios of 0.173, 0.337 and 0.5 using FLUENT. His results show that the flow separation is delayed and the ratio of lift to drag is increased at the slot location of 10% of the chord length and the suction ratio of 0.5. The flow remains attached at the upper surface of the aerofoil up to the high angle of attack of 21 degrees. In both of Godarzi works, the incompressible flow was assumed and no transition criterion was used. The overall purpose of this study is to examine several examples of laminar flow control especially over the aerofoil surfaces with a desired flow control technique. Thus, the surface suction is applied to delay the flow transition point from laminar to turbulent and also to maximize the lift to drag ratio. The effects of design parameters such as the suction slot location, suction inclination angle and the extent of sucked flow through slots are investigated. For this purpose, it is required to solve flow field equations and determine the transition location point accurately. In this paper, an implicit, time marching, high resolution total variation diminishing (TVD) scheme of Sedaghat [10] is used to solve the governing two-dimensional Navier-Stokes equations. To determine the transition location point, the e^N method is employed. Then, the stability analysis is conducted by solving the Orr-Sommerfeld equation. Next with the e^N method, the location of transition point is determined. Finally, the flow field is solved in both laminar and turbulent regimes independently. The results are presented for several examples of active flow control.

This paper is organized as follows: Section 2 gives a brief account on methodology. In this section, fluid flow equations, turbulence modelling and surface mass transfer effects and modelling flow

instabilities for determining onset of transition are described. Numerical method included shock wave control for VFW-VA-2 aerofoil in transonic flow, transition control for NACA65_3-018 aerofoil in subsonic flow, effect of suction slot location are discussed in section 3. Effect of suction inclination angle and effect of suction strength are investigated as well. In section 4 conclusions are drawn.

2. THE GOVERNING FLUID FLOW EQUATION

Neglecting body forces and volumetric heating, non-dimensional form of compressible Navier-Stokes equations in the general curvilinear coordinate system for two dimensional fluid flows can be written as:

$$\frac{\partial \hat{U}}{\partial t}+\frac{\partial \hat{F}}{\partial \xi}+\frac{\partial \hat{G}}{\partial \eta}=0 \tag{1}$$

Where $\hat{U}=U/J$, $\hat{F}=(\xi_x F+\xi_y G)/J$, $\hat{G}=(\eta_x F+\eta_y G)/J$, $J=\xi_x\eta_y-\xi_y\eta_x$. Also $\xi=\xi(x,y)$ and are $\eta=\eta(x,y)$ coordinate transformation functions, $\xi_x, \xi_y, \eta_x,$ and η_y are metrics and are derivatives of ξ and η with respect to x and y, respectively. J is Jacobian of the transformation. The vectors U, F and G are given by:

$$U=\begin{bmatrix}\rho\\ \rho u\\ \rho v\\ e\end{bmatrix},\quad F=\begin{bmatrix}\rho u\\ p+\rho u^2-\tau_{xx}\\ \rho uv-\tau_{xy}\\ (e+p)u-u\tau_{xx}-v\tau_{xy}+q_x\end{bmatrix},\quad G=\begin{bmatrix}\rho v\\ \rho uv-\tau_{xy}\\ p+\rho v^2-\tau_{yy}\\ (e+p)v-u\tau_{xy}-v\tau_{yy}+q_y\end{bmatrix} \tag{2}$$

where ρ, p, u, v, e and q are density, pressure, velocity components along x, y directions, total energy per unit volume, and heat flux respectively. The components of shear stress tensor are expressed as a function of viscosity μ, the Reynolds number Re and derivatives of velocity components as $\tau_{xx}=\frac{\mu}{\mathrm{Re}}\left(\frac{4}{3}\frac{\partial u}{\partial x}-\frac{2}{3}\frac{\partial v}{\partial y}\right),\tau_{yy}=\frac{\mu}{\mathrm{Re}}\left(\frac{4}{3}\frac{\partial v}{\partial y}-\frac{2}{3}\frac{\partial u}{\partial x}\right)$ and $\tau_{xy}=\frac{\mu}{\mathrm{Re}}\left(\frac{\partial u}{\partial y}+\frac{\partial v}{\partial x}\right)$.

The Navier-Stokes (NS) equations which govern conservation laws, i.e. conservation of mass, momentums and energy, are written in curvilinear system so that they can be easily adopted for solving flow field around any curved geometries. The NS equations in non-dimensional form (above) are then solved in a uniformly spaced rectangular computational domain obtained from any physical mesh in 2D geometries. In fact, computational domain is a rectangular uniformly spaced which is the result of general coordinate transformation from optional 2D physical domain into computational domain. The free stream values of primitive variables are used to make dimensionless equations [10].

2.1. Turbulence Modelling and Surface Mass Transfer Effects

For laminar and compressible flows, the coefficient of viscosity μ, is obtained from molecular viscosity coefficient by Sutherland's law as:

$$\frac{\mu_l}{\mu_\infty}=\left(\frac{T}{T_\infty}\right)^{3/2}\left(\frac{T_\infty+S}{T+S}\right) \tag{3}$$

where S = 110.4 is Sutherland's law coefficient. For turbulent flow, the coefficient of viscosity in equations (2) is replaced by $\mu=\mu_l+\mu_t$. Where turbulent viscosity coefficient μ_t is determined using the algebraic eddy-viscosity model proposed by Baldwin and Lomax. This well-known model is widely used in aeronautical field. It is a two-layer model based on Prandtl's mixing length concept explained in detail in [10]. The effect of mass transfer at the wall is modelled in Baldwin-Lomax (1978) turbulence model using modification to Van Driest factor (A^+). Changing in A^+ is firstly proposed by Cebeci [11] and then modified by Chokani and Squire [12] is presented as follows:

$$A^+ = 26\left\{\exp\left(11.8v_w^+\right) - \frac{p^+}{v_w^+}\left[\exp\left(11.8v_w^+\right) - 1\right]\right\}^{-\frac{1}{2}} \tag{4}$$

in which v_w is suction speed at the wall and

$$p^+ = \frac{-\mu_w}{\mathrm{Re}_\infty \rho_w^2 u_\tau^3}\left(\frac{dp}{d\xi}\right)_w \quad v_w^+ = \frac{v_w}{u_\tau} u_\tau = \sqrt{\frac{\tau_w}{\rho_w}} \tag{5}$$

where μ_w and ρ_w is molecular viscosity and density at the wall, Re is free stream Reynolds number, $(dp/d\xi)_w$ is pressure gradient in the stream wise direction at the wall, u_τ is friction velocity and τ_w is shear stress at the wall.

2.2. Modelling Flow Instabilities for Determining Onset of Transition

The e^N method is a semi-empirical method based on linear stability theory which uses the solution of Orr-Sommerfeld equation for determining onset of transition location from laminar to turbulent regime (see Cebeci et al 2005). The Orr-Sommerfeld equation is an approximation to perturbed form of the governing NS equations for determining amplitude's amplification or decay of a disturbance in parallel flows. Utilizing linear stability theory and assuming small disturbances, a stream function for the disturbances may be introduced by $\psi(x, y, t) = \phi(y) \exp[i(\alpha x - \omega t)]$. Where $i = \sqrt{-1}$ is the complex number, α $(= \alpha_r + i\alpha_i)$ is a dimensionless wave number and ω $(= \omega_r + i\omega_i)$ is dimensionless frequency of the disturbances. The Orr-Sommerfeld equation for the complex amplitude $\phi(y)$ is derived due to boundary conditions as follow:

$$\begin{aligned}
&\left(u = \frac{\omega}{\alpha}\right)\left(D^2 - \alpha^2\right)\phi(y) - \frac{d^2u}{dy^2}\phi(y) = \frac{-i}{\alpha\,\mathrm{Re}_\infty}\left(D^4 - 2\alpha^2 D^2 + \alpha^4\right)\phi(y) \\
&y = 0,\ \phi = 0,\ \phi' = 0 \\
&y = \delta,\ (D+\sigma)(D+\alpha)\phi = 0 \\
&y = \delta,\ (D+\sigma)(D^2 - \alpha^2)\phi = 0
\end{aligned} \tag{6}$$

where D is differentiation operator with respect to $y = y^*/\delta^*$, $u(y)$ is x-component of velocity in boundary layer, δ is boundary layer thickness, and $\sigma^2 = \alpha^2 + i\,\mathrm{Re}(\alpha u - \omega)$. Note that the Orr-Sommerfeld equation is expressed in dimensionless form using velocity at the edge of boundary layer, U_e^* and boundary layer displacement thickness, δ^*. Therefore, the dimensionless wave number α and frequency ω are expressed based on dimensional quantities (with superscript asterisk) as $\alpha = \alpha^*\delta^*, \omega = \dfrac{\omega^*\delta^*}{U_e^*}$.

In this research, an efficient finite difference method is used for solving eigenvalue problem to obtain the solution to Orr-Sommerfeld equation. The numerical algorithm can be found in Cebeci [11]. The method is highly dependent on an initial estimation for required parameters and in case of bad guess the method may diverge. To overcome the problem, some artifices are adopted including Newton iteration method for solving non-linear equations and a relation specified to compute initial values from pervious grid point values [11, 13].

Now, with availability of eigenvalues of Orr-Sommerfeld equation, the location of transition can be determined using e^N method. The basic assumption in this method is that transition starts when a small disturbance is introduced at a critical Reynolds number and is amplified by a factor of e^N which, is about 8000 for a typical value of N equal to 9. The value of N in a typical flow may be specified from experimental tests. The calculation of transition with this procedure is relatively straight-forward in two-dimensional flows. After finding the eigenvalues of Orr-Sommerfeld equation, amplification rates $(-\alpha_i)$ as a function of s (or Re) for a range of dimensional frequencies ω^* are available (s is the distance of points on airfoil surface measured from the stagnation point). At this step, the amplification factor (N),

can be calculated by $N = \int_{s_{ne}}^{s} -\alpha_i(\omega)ds$. Where s_{ne}, corresponds to each value of s on neutral stability curve. This procedure is repeated for several lines of constant frequency. These constant frequency. These constant frequency lines are effective in stability analysis procedure because trajectory of a single disturbance in a constant frequency in several velocity profiles is analyzed. Then, curves of amplification factor (N) with respect to s (or Re) are generated for each constant frequency in a graph. The maximum of those curves which corresponds to maximum amplification factors displays the parameter s (or Re) for transition point from which is computed with a value for N, specified from experimental results. The value of N at transition onset should be determined in wind tunnel experiments. Mack [14] suggested an empirical relation due to a correlation from the analysis of Dryden's measurements for computing N-factor at transition onset as a function of free stream turbulence intensity (Tu) as $N = -8.43–2.4$ ln(Tu). The total disturbance level in a wind tunnel is affected by both turbulence and sound. Below $Tu = 0.1\%$, the sound component controls transition. As a result, decreasing turbulence component only decreases the signal registered by a hot-wire anemometer without affecting transition Reynolds number. The effect of free stream turbulence on transition is given by the mentioned relation for $Tu > 0.1\%$ [14]. Moreover, Van Ingen [15] suggested a similar relationship to that of Mack relation. He declared that for values of $Tu < 0.1\%$, there is a considerable scatter in the experiments because in this region acoustic fluctuations may control transition rather than turbulence. So, the aforementioned relations are useful for turbulence level above 0.1%. For $Tu < 0.1\%$, an "effective" value for Tu should be defined. It should be mentioned that the free stream turbulence level is not sufficient to describe the disturbance. Information about distribution across the frequency spectrum should also be available. In addition to turbulence levels, the acoustic disturbances are important. In this case, the most important issue is "receptivity": how the initial disturbances within the boundary layer are related to the outside disturbances. Therefore the relationships for specifying the "critical N-factor" can only be used if an "effective Tu" is known. This effective turbulence level can only be determined through a comparison of measured transition positions with calculated amplification ratios. In fact, it has become customary to define the quality of a wind tunnel by stating its "critical N-factor" [15].

In this paper for transition prediction with the e^N method, the value of $N = 9$ is selected for the flow around 2D aerofoil sections in wind tunnels with turbulent intensity levels less than 0.1%. This is mostly because of comparing the results with experimental data. These data are from Gregory et al. (1970) and some researchers who suggested this value for the flow around 2D aerofoils in wind tunnels with $Tu < 0.1\%$ like Cebeci [11, 16 and 17].

3. NUMERICAL EXAMPLES AND DISCUSSION

The methods and theories of transition prediction and fluid flow solver are discussed. Here, the results are given for flow control process and optimization procedure used to measure the effects of some parameters on surface suction.

3.1. Shock Wave Control for VFW-VA-2 Aerofoil in Transonic Flow

The two-dimensional supercritical VFW-VA-2 aerofoil with maximum thickness of 13% was tested extensively by Krogmann [18] in the DFVLR 1 m ∞ 1 m transonic wind tunnel, which is a closed circuit continuous tunnel. The free stream flow conditions chosen for present computation are Re = 2.4 ∞ 10^6, Ma = 0.78 and AOA = 4° corresponding to one of the wind tunnel experiments. In this experiment, the slotted region was located between 55% and 62.5% of chord length from the leading edge of the aerofoil upper surface, which was downstream of the shock position. The computational grid was a 230 ∞ 135 C-type hyperbolic mesh. The increment of nodes in stream wise direction was due to clustering points in the suction region to improve accuracy of results. A suction coefficient of 0.0006 was used for controlling the induced separation due to shock-boundary layer interaction, where the suction coefficient is defined as [1]:

$$C_Q = \frac{\int_{\xi 1}^{\xi 2} \rho_w(-U_Q)d\xi}{\rho_\infty U_\infty c} \tag{7}$$

where U_Q is the suction velocity within the suction slot ($\xi_1 < \xi < \xi_2$).

Figure 1 shows the pressure distributions over the aerofoil surfaces for two cases; (a) no suction and (b) suction case. For the aerofoil upper surface, comparison with experimental data is also presented in Figure 1. The experimental data was only available for the upper surface. The effects of the surface suction are captured relatively well. For the two cases, there is a good agreement between present results and those of experiment. Only some discrepancy is observed around the shock position, which may exhibit lower accuracy of the computation for capturing this region with very high gradient of flow.

For the effect of boundary layer suction on the flow features, it is observed that a steep pressure rise can be observed in suction region in both experimental and computational results. It is also can be seen that the shock position is moved downstream in the suction flow case (Figure 1c). In fact, the shock location has been determined as the mid-point of the region where the discontinuity in pressure coefficient occurs, according to Ref. [18]. For the transonic cases presented in Fig. 1, the shock locations are at 0.52c and 0.57c for solid and suction conditions, respectively.

From the Mach and iso-pressure contours in Figure 2, more insights to the transonic flow domain can be gained. Firstly, a closer look at Fig. 2 would confirm the findings regarding the shock location. Moreover, the delay in shock location due to active suction, however small, can be observed from these graphs. This delay in shock location by suction results in a smaller subsonic region downstream of the shock position. Moreover, it is well known from the literature that the flow downstream of the shock location over transonic aerofoils is separated due to stationary or rapidly growing shock-induced separation bubbles [19, 20]. This means that shock-induced separation due to shock phenomena is delayed increasing lift and reducing wave drag using surface suction control. It should be noted that the values of iso-pressure contours displayed in Figure 2 are presented in dimensionless form as:

$$P = \frac{P^* / P_\infty}{\gamma M_\infty^2} \tag{8}$$

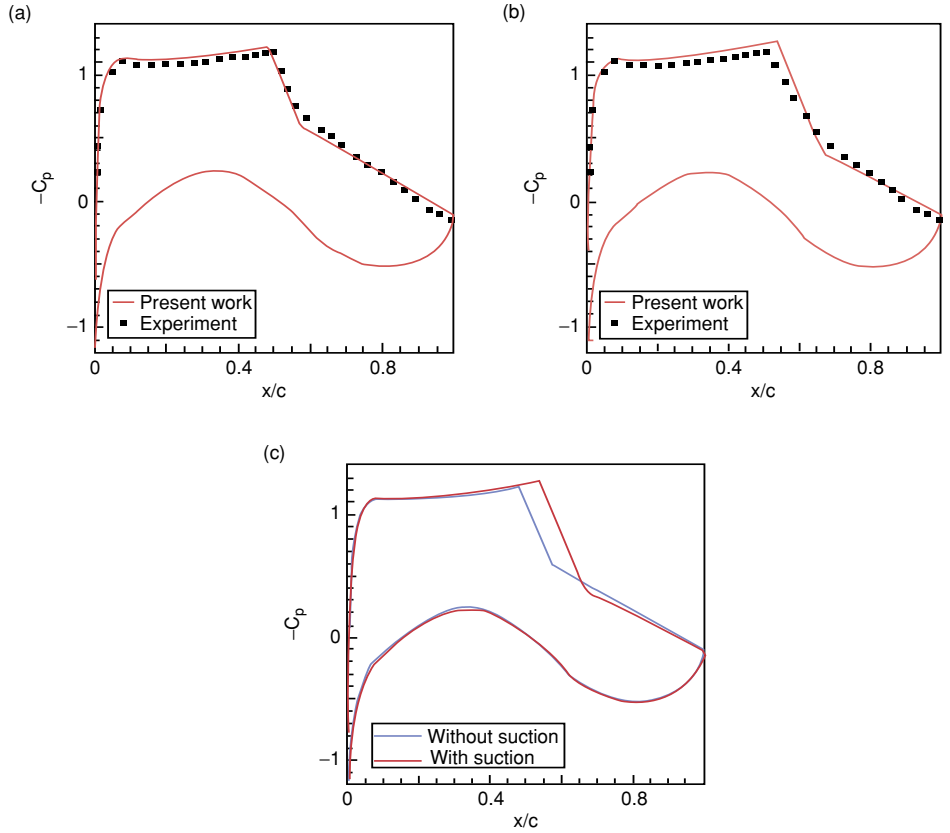

Figure 1. Pressure distributions over the VFW-VA-2 aerofoil surfaces, (a) flow without suction, (b) flow with suction, (c) flow with and without suction; slot position: (0.55c–0.625c), $C_Q = 0.0006$.

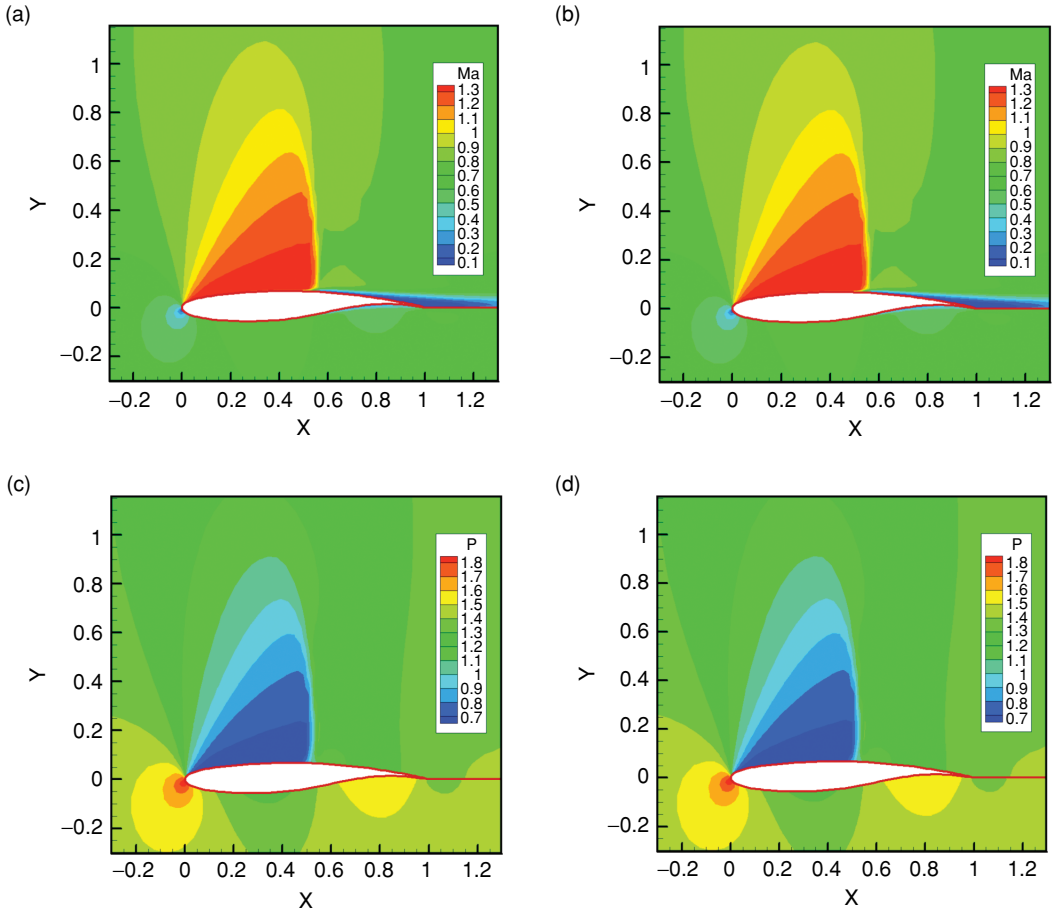

Figure 2. Flow field solutions for the VFW-VA-2 aerofoil (a) Mach contours for no-suction case, (b) Mach contours for suction case, (c) iso-pressure contours for no-suction case, (d) iso-pressure contours for suction case.

To improve the results close to shock region, mesh points are clustered in the suction region as shown in Figure 3a. In Figure 3b, details of the suction velocity vectors and the flow streamlines within the suction region for VFW-VA-2 aerofoil are displayed.

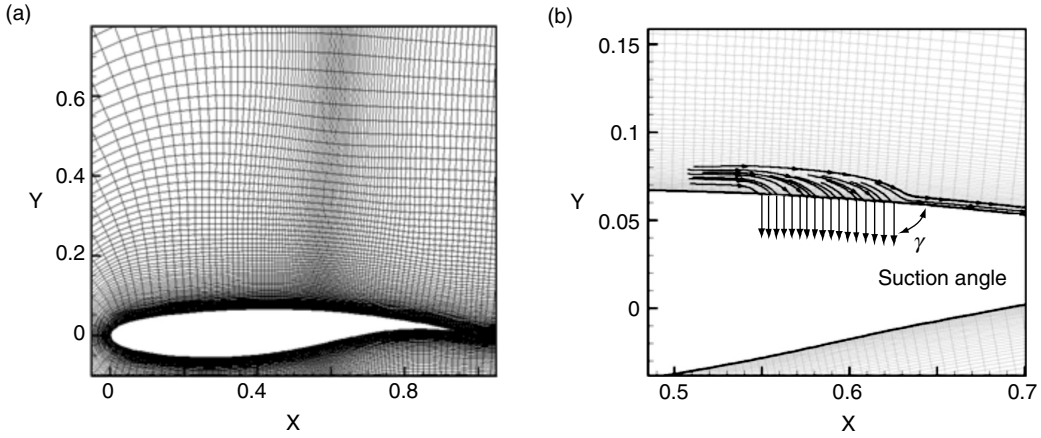

Figure 3. Mesh and flow details close to suction region for the VFW-VA-2 aerofoil; (a) Mesh clustering in the vicinity of suction slot (0.55c–0.65c), (b) Sucked velocity vectors and flow streamlines within the slotted region.

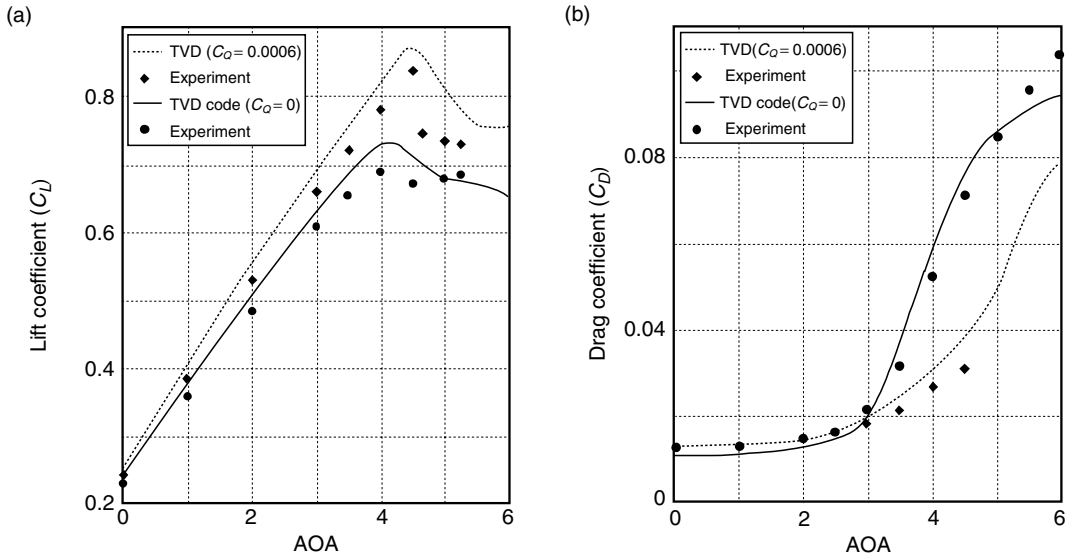

Figure 4. Lift and drag coefficients for VFW-VA-2 aerofoil; (a) no-suction ($C_Q = 0$) (b) suction ($C_Q = 0.0006$) instances.

The effects of local boundary-layer suction on the aerodynamic performance of the VFW-VA-2 aerofoil are demonstrated in Figure 4 using lift and drag coefficients versus angle of attack with and without suction. It can be seen that lift coefficient is enhanced for all incidence angles using tiny suction coefficient of $C_Q = 0.0006$. Remarkably, the computational results are in a very good agreement with experimental data for both cases (no suction and suction cases) up to incidence angle of AOA = 4°. For AOA > 4°, there are some discrepancies because of flow separation between present results and experimental data as can be seen in Figure 4. Another effect of suction observed in Figure 4 is that the stall angle for the suction case increases compared with no-suction. It should be noted that the VFW-VA-2 aerofoil is categorised as thin aerofoil with corresponding thin aerofoil stall at low stall incidence angle [23]. Drag coefficient is also favourably reduced using tiny suction as revealed in Figure 4.

This is particularly significant because the suction region is considerably reduced drag coefficient for incidence angles higher than 3 degrees. But for AOA < 3°, there are few advantages on drag reduction. Moreover, a very good agreement is observed between the numerical results and experimental data. However, experimental data is only available for the suction case between the incidence angles 2 and 4.5 degrees.

3.2. Transition Control for NACA65$_3$-018 Aerofoil in Subsonic Flow

The surface suction is applied to control transition point from laminar to turbulent regime over NACA65$_3$-018 aerofoil. A case study is carried out to investigate the effects of different factors such as suction slot location, suction inclination angle and extent of sucked flow through slots for the flow on the upper surface. This is a low-drag aerofoil also called fat aerofoil with maximum thickness to chord ratio of 18% [22-23]. The free stream flow conditions applied for this condition are Re = 3 ∞ 10^6, Ma = 0.22 and AOA = 1.5°.

3.2.1. Effects of Suction Slot Location

To investigate the effects of suction slot location on flow control over NACA653-018 aerofoil, seven positions are used on the upper aerofoil surface to implement a suction slot. The length of suction slot is considered to be 3% of the chord length. Computational grid is a 211 ∞ 131 C-type hyperbolic mesh. The increment of nodes in stream wise direction is due to clustering points in the suction region to improve accuracy of results. For all seven instances, the flow field is solved around the aerofoil section using the flow solver [10] and transition point is simultaneously determined using e^N method. Figure 5 shows the results for transition location, lift and drag coefficients using three suction coefficients, C_Q = 0.0001, 0.0005, and 0.001. For no suction case, the values for these parameters are x_{tr} = 0.388c, C_L = 0.18 and C_D = 0.005. In all slot locations, transition is delayed, lift coefficient is increased and drag

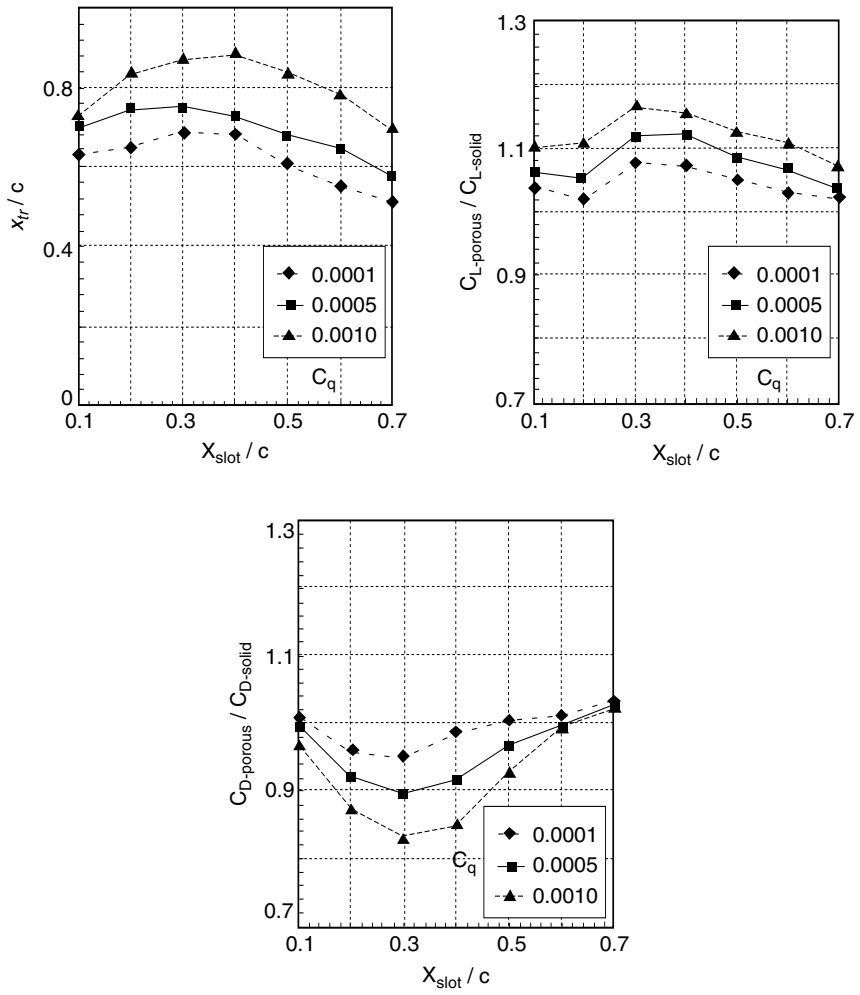

Figure 5. (a) Effect of suction slot position on transition location, (b) Effect of suction slot position on lift coefficient, (c) Effect of suction slot position on drag coefficien.

coefficient is decreased except for a few instances. For higher suction coefficients, transition occurs further downstream and more lift enhancement and drag reduction are observed. It is observed that the optimum location for suction slot is about 30% of the chord length (Figure 5). Moreover, if it is considered that transition point for no suction case occurs at 38.8% of the chord length, it is realized that a suitable location for the slot is upstream of the transition point. Besides, form stability analysis viewpoint, it is known that the critical point lies upstream of transition point. Therefore, it seems that the gap between critical point and the transition point is a suitable location for applying suction region, because at this gap the flow disturbances grows rapidly.

3.2.2. Effect of Suction Inclination Angle

To find the most suitable suction inclination angles, the approach is repeated for three inclination angles of 30, 60 and 90 degrees for all positions using the suction coefficient value of 0.001. The suction inclination angle (γ) is the angle between aerofoil surface and suction velocity as specified in Figure 3b. The results are reproduced in Figure 6 for the transition location, lift and drag coefficients. It is observed that the suction inclination angle of $\gamma = 90°$ is the best choice due to a better delay in transition, lift enhancement and drag reduction. This is also observed by other researchers [5].

3.2.3. Effect of Suction Strength

To study suction strength effects, the suction coefficient is varied using four suction coefficients of 0.0000, 0.0001, 0.0005 and 0.0010. Figure 7 shows the effects of suction strength on lift to drag ratio at five incidence angles of 2, 6, 10, 14, and 18 degrees. The suction slot is situated at a distance on the

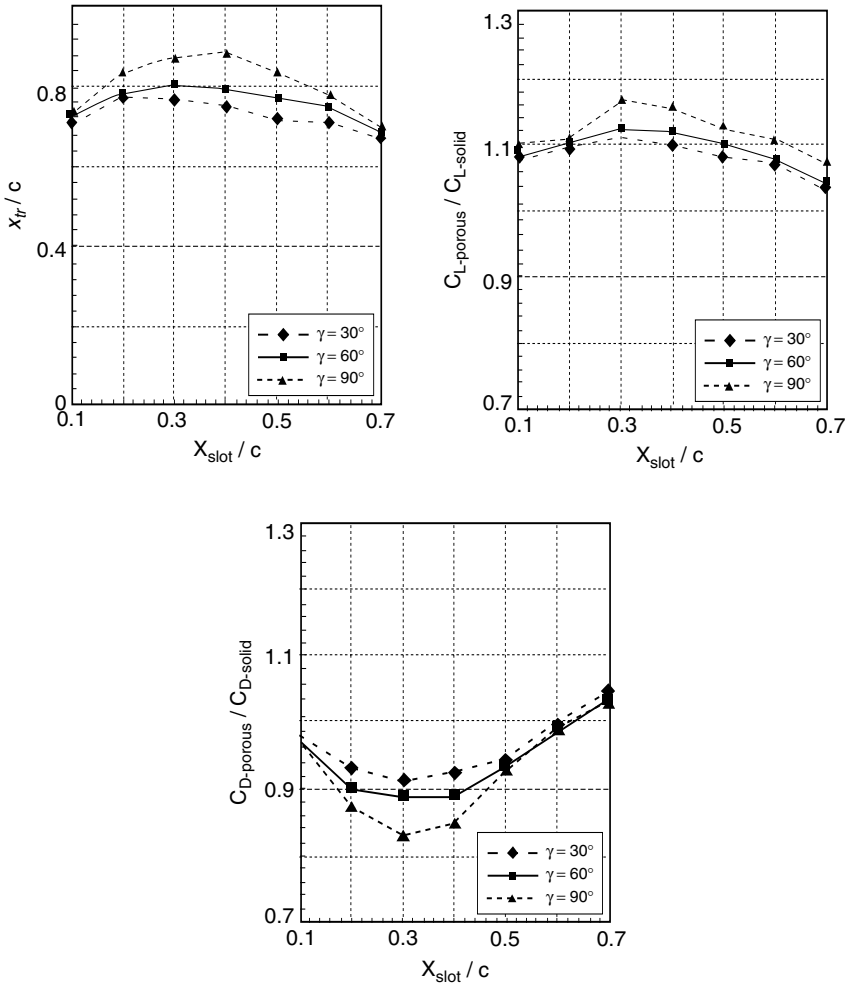

Figure 6. (a) Effect of suction inclination angle on transition location (b) Effect of suction inclination angle on lift coefficient (c) Effect of suction inclination angle on drag coefficient.

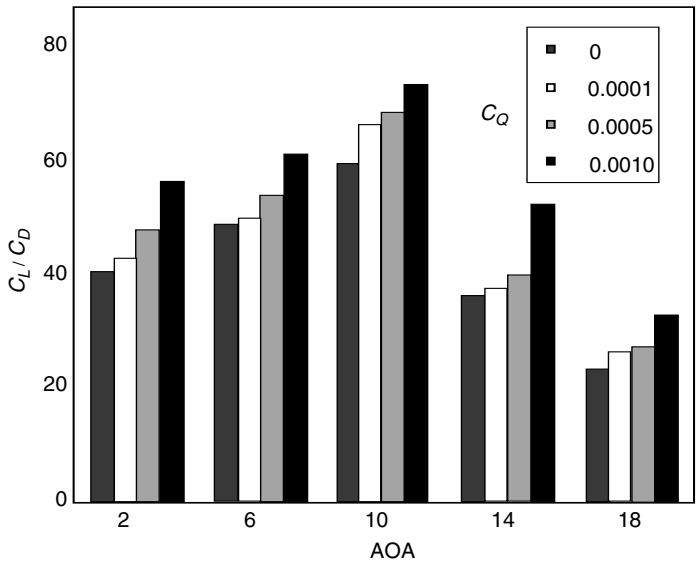

Figure 7. Lift to drag ratio variations versus AOA using different suction coefficients.

upper aerofoil surface at approximately 30% of the chord length (between 28.5 and 31.5% chord length).

The aforementioned values for suction coefficient are selected in such a way that suction effects appeared only within the boundary layer. In fact, in some works, the suction affects the whole flow (within and outside the boundary layer), but this paper seeks to analyse the effect of suction only within the boundary layer. Therefore, the suction velocity is adopted to be less than y-component of flow velocity in the boundary layer. Moreover, from the boundary layer scale analysis, y-component of flow velocity in the boundary layer was found to be about less than 5% of the free stream velocity (the maximum of x-component of flow velocity in boundary layer). From Figure 7, it can be seen that for low values of suction coefficient there is only a small increase in lift to drag ratio except for AOA = 10°. However, with higher values of suction coefficient lift to drag ratio increases considerably. Furthermore, in case of $C_Q = 0.0010$, maximum enhancement of the value of lift to drag ratio occurs at incidence angle of 14 degrees. This indicates that stronger suction may improve the aerofoil performance at high incidence angles. One of the undesirable effects of flow in high angles of incidence is flow separation which may be tackled using surface suction [6, 24].

To explain the suction effects on flow stability, velocity profiles within the boundary layer has to be examined. As shown in Figure 8, boundary layer velocity profiles are compared before and after the suction slot for with and without suction. Suction coefficient is 0.0010 and suction slot is situated at 30 percent of the chord length on upper aerofoil surface. Figure 8a shows velocity profiles before suction slot for both with and without suction flows. As observed, the suction velocity profile looks like a fuller profile as profiles with favourable pressure gradient. These types of profiles have a large curvature, so

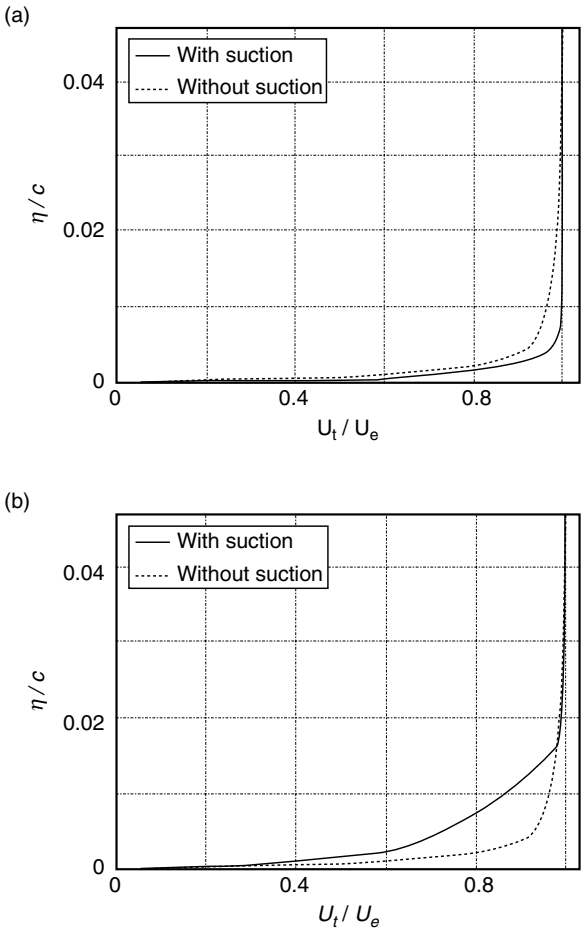

Figure 8. Boundary layer velocity profiles, (a) prior to the suction slot (at distance 0.283c), (b) just after the suction slot (at distance 0.317c).

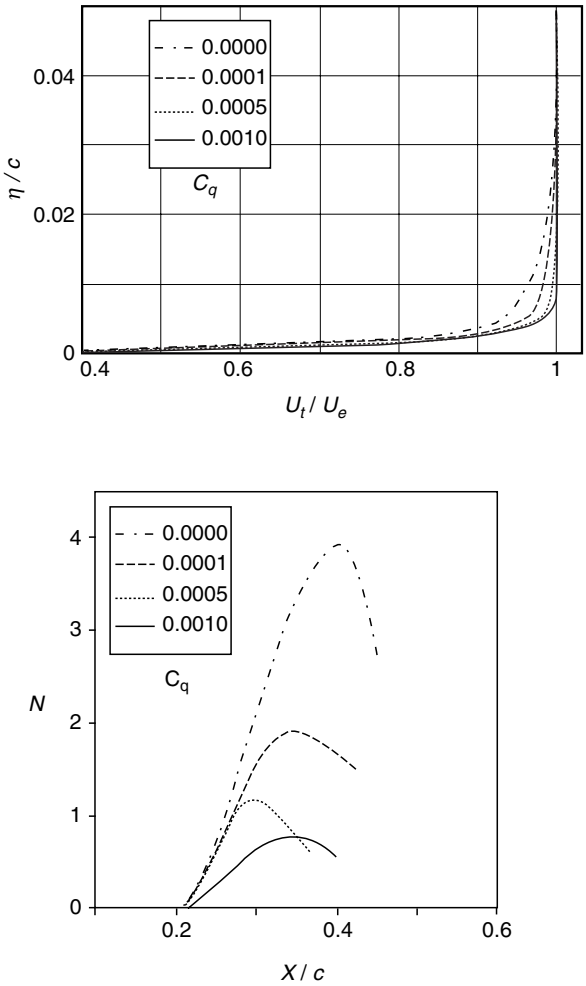

Figure 9. Effects of suction coefficient on boundary layer stability, (a) boundary layer velocity profiles, (b) spatial amplification factor, N, values.

they have more stability limit (larger critical Reynolds number) than profiles without suction according to stability analyses. The change in suction profile is due to the fact that, with suction the fluid particles are sucked in to the suction chamber.

It is obvious that the fluid particles which are nearer to the wall have a greater chance to be sucked in than the further ones. So, the closest molecules and eddies to the surface which have lower speed and energy, are replaced with particles with higher speed and energy from farther distances from the wall. Hence, at a specified distance from the wall, fluid particles in suction flow have a greater speed in comparison with no-suction flow. These points explain why velocity profiles of flow with suction are fuller than velocity profiles of flow without suction.

Figure 8b is related to velocity profiles just after end of the slot. Since the continuity of boundary layer is removed due to suction, a new boundary layer forms which starts from the final edge of the suction slot. So, because of high normal velocity at this section, the velocity profile has a sharper form at the bottom, but gradually its form changes to its normal shape under the influence of viscosity.

Effects of suction coefficient on boundary layer stability are observed in Figure 9. Velocity profiles are presented for three different suction coefficients just before the slot suction at 0.2c (Figure 9a). The slot suction is situated at 30% of the chord length. From this figure, it is observed that the boundary layer profiles become fuller as the suction coefficient increases. Stability flow analyses as shown in Figure 9b, confirms more stable flow and less amplification factor for higher suction coefficient. According to the flow stability theories [14, 15], the disturbances trying to advance transitional process do not get enough amplification ($N < 9$), and therefore the transition from laminar to turbulent regime cannot be completed, even though the transition process was already started. It should be recalled that

the flow cases studied in Fig. 9b are corresponding to the flow around a $NACA65_3$-018 aerofoil at a very low angle of attack of AOA = 1.5°, and moderate Reynolds number of Re = 3 ∞ 10^6. The aerofoil flows at low angles of attack are likely to be non-separated. Moreover, considering the fact that the slot suction is situated at 30% of the chord length would indicate that the boundary layer formed in the region of 0 < x < 0.3c is sucked to the suction chamber and a new boundary layer is formed downstream this location. The evidences stated above would imply that an attached laminar stable flow is most likely to occur in these cases. It should also be remarked here that the effect of local Reynolds number is weekend since the new boundary layer is not formed from the aerofoil leading edge.

4. CONCLUSION

In this paper, the e^N method which uses the solution of Orr-Sommerfeld equation is employed together with a high resolution TVD numerical solver for determining onset of transition location from laminar to turbulent regime by solving the compressible Navier-Stokes fluid flow equations.

The two-dimensional supercritical VFW-VA-2 aerofoil with maximum thickness of 13% was studied at the free stream flow conditions of Re = 2.4 ∞ 10^6, Ma = 0.78 and AOA = 4°. It is observed that the shock position is moved downstream employing a suction coefficient of 0.0006. In the suction case, a steep pressure rise can be observed in suction region in both experimental and computational results. It is also observed that the shock position with suction condition is located further downstream and the supersonic region is extended on aerofoil upper surface. This means that shock-induced separation due to shock phenomena is delayed, the lift enhanced and the wave drag reduced.

The effects of local boundary-layer suction on the aerodynamic performance of the VFW-VA-2 aerofoil are demonstrated. It was observed that lift coefficient is enhanced for all incidence angles using tiny suction coefficient of C_Q = 0.0006. Remarkably, the computational results are in a very good agreement with experimental data for both cases (no suction and suction cases) up to incidence angle of AOA = 4°. For AOA > 4°, there are some discrepancies between present results and experimental data because of flow separation.

The surface suction is applied to control transition point from laminar to turbulent regime over $NACA65_3$-018 aerofoil. A case study is carried out to investigate the effects of different factors such as suction slot location, suction inclination angle and extent of sucked flow through slots for the flow on the upper surface. In all slot locations, transition is delayed, lift coefficient is increased and drag coefficient is decreased except for a few instances. It is observed that the optimum location for suction slot is about 30% of the chord length when transition occurs, at 38.8% of the chord length. It is observed that the suction inclination angle of $\gamma = 90°$ is the best choice due to a better delay in transition, lift enhancement and drag reduction. The stronger suction may improve the aerofoil performance at high incidence angles when flow separation occurs.

REFERENCES

[1] Gad-el-Hak, M., *Flow Control: Passive, Active, and Reactive Flow Management*, Cambridge University Press, Cambridge, 2000.

[2] Braslow, A.L., *A history of suction type LFC with emphasis on flight research*, Monographs in aerospace history no. 13, NASA, 1999.

[3] Balakumar, P. and Hall, P., Optimum suction distribution for transition control, *Journal of Theoretical and Computational Fluid Dynamic* 13, 1999, 1–19.

[4] Bobbitt, P.J., Ferris, J.C., Harvey, W.D. and Goradia, *S.H., Hybrid laminar flow control experiment conducted in NASA Langley* 8*-foot transonic pressure tunnel*, NASA TP-3549, 1996.

[5] Huang, L., LeBeau, R.P., Huang, P.G. and Hauser, T., *Optimization of blowing and suction control on NACA0012 aerofoil using genetic algorithm*, 42th AIAA Aerospace Sciences Meeting and Exhibit, Reno, Nevada, AIAA paper 2004, 22.

[6] Atik, H., Kim, C.Y., Van Dommelen, L.L. and. Walker, J.D.A., Boundary-layer separation control on a thin airfoil using local suction, *Journal of Fluid Mechanic* 535, 2005, 415–443.

[7] Pralits, J.O., and Hanifi, A., *Optimal suction design for hybrid laminar flow control, sixth IUTAM Symposium on Laminar-Turbulent Transition*, Springer, Netherlands, 2006, 201–206.

[8] Goodarzi, M., Rahimi, M., and Fereidouni, R., Investigation of Active Flow Control over NACA0015 Airfoil Via Blowing, *International Journal of Aerospace Sciences*, 1(4), 2012, 57–63.

[9] Goodarzi, M., Fereidouni, R., and Rahimi, M., Investigation of flow control over a NACA 0012 aerofoil by suction effect on aerodynamic characteristics, *Canadian Journal on Mechanical Sciences & Engineering*, 3(3), 2012.

[10] Sedaghat, A., *A finite volumeTVD approach to Transonic Flow Computation*, PhD Thesis, The University of Manchester, UK, 1997.

[11] Cebeci, T., Shao, J.P., Kafyeke, F. and Laurendeau, E. *Computational Fluid Dynamics for Engineers*, Horizons Publishing, California, 2005.

[12] Chokani, N. and Squire, L.C. Transonic shockwave/turbulent boundary layer interactions on porous surface, *Aeronautical Journal*, 1993, 163–170.

[13] Ng, B.S. and Reid, W.H. On the Numerical Solution of the Orr-Sommerfeld Problem: Asymptotic Initial Conditions for Shooting Methods, *Journal of Computational Physics* 38, 1980, 275–293.

[14] Mack, L.M. *Transition and Laminar Instability*, Jet Propulsion Laboratory Publication 77–15, Pasadena, CA, 1977.

[15] Van Ingen, J.L. *The e^N method for transition prediction, Historical review of work at TU Delft*, 38th AIAA Fluid Dynamics Conference and Exhibit, Seattle, Washington, AIAA paper, 2008, 2008–3830.

[16] Stock, H.W. and Haase, W. Feasibility Study of eN Transition Prediction in Navier–Stokes Methods for Airfoils, *AIAA Journal* 37(10), 1999, 1187–1196.

[17] Crouch, J.D., Crouch, I.W.M. and Ng, L.L. Transition Prediction for Three-Dimensional Boundary Layers in Computational Fluid Dynamics Applications, *AIAA Journal* 40(8), 2002, 1536–1541.

[18] Krogmann, P., Stanewsky, E., and Theide, P. Effect of Suction on Shock/Boundary-Layer Interaction and Shock-Induced Separation, *Journal of Aircraft*, 22(1), 1985, 37–42.

[19] Shahneh, A.Z. and Motallebi, F., Effect of submerged vortex generators on shock-induced separation in transonic flow, *Journal of Aircraft*, 46(3), 2009, 856–863.

[20] Sartor, F., Losfeld, G. and Bur, R., PIV study on a shock-induced separation in a transonic flow, *Experiments in Fluids*, 53(3), 2012, 815–827.

[21] Gad-el-Hak, M., Control of low-speed airfoil aerodynamics, *AIAA Journal*, 28(9), 1990, 1537–1552.

[22] Nelson, P.A., Wright, M.C.M. and Rioual, J.L., Automatic control of laminar boundary-layer transition, *AIAA Journal* 35(1), 1997, 85–90.

[23] Racisz, S.F., *Experimental investigation of the effectiveness of various suction-slot arrangements as a means for increasing the maximum lift of the NACA*65_3-018 *aerofoil section*, NACA RM L50A10, 1950.

[24] Wahidi, R. and Bridges, D.H., *Control of laminar separation bubbles with distributed suction: preliminary studies*, 46th AIAA Aerospace Sciences Meeting and Exhibit, Reno, Nevada, AIAA paper, 2008, 738.